PERGAMON

Chemical Engineering Science 54 (1999) 2295–2303

Chemical Engineering Science

Impact of an undesired reaction on a boiling slurry reactor

J. Khinast[a,*], D. Luss[a], T.M. Leib[b], M.P. Harold[c]

[a]*Department of Chemical Engineering, University of Houston, Houston, TX 77204-4792, USA*
[b]*DuPont Engineering, Wilmington, DE 19880-0304, USA*
[c]*DuPont Dacron®, Wilmington, DE 19880-0304, USA*

Abstract

We study the impact of an undesired simultaneous or consecutive exothermic reaction on the behavioral feature of a boiling slurry reactor (BSR). The BSR is fed by a solution of a non-volatile liquid reactant and a gaseous reactant, while the effluent consists only of gas. While, the BSR can have only a unique steady state if a single reaction occurs, the undesired reaction may lead to the existence of multiple steady states. A unique feature of the BSR is the possible existence of fill-up and dry-up states at which the reactor volume changes monotonically while the other state variables remain unchanged. The fill-up state will lead to spillover unless the feed conditions are properly adjusted. An undesired consecutive reaction leads to more intricate dynamic features than does a simultaneous undesired reaction.

Keywords: Boiling slurry reactor; Gas–liquid reaction; Multiplicity; Dynamics; Reaction networks

1. Introduction

Slurry reactors involve reactions of a gas-phase and a liquid-phase reactant with a solid catalyst. Recent reviews of these reactors were presented by Shah (1979), Ramachandran and Chaudhari (1983), Gianetto and Silveston (1986), Fan (1989), Hammer et al. (1984), Beenackers and van Swaaij (1986), and Krishna and Ellenberger (1995). In a boiling slurry reactor (BSR) the reaction heat is removed by condensation of an evaporating reaction mixture. Luyben (1966) noted that a closed loop control may be needed for stable operation of a BSR. Several important commercial processes such as C_4-alkylation and synthesis of tetraethyl lead and polyethylene utilize a BSR.

We consider here a special configuration of a BSR, in which a non-volatile liquid reactant, dissolved in a volatile solvent reacts with a gaseous reactant. The effluent consists only of gases. This operation is illustrated in Fig. 1. Potential applications encompass exothermic gas–liquid reactions for which the reaction products are much more volatile than the liquid reactant, for example the hydrogenation of pyrrole (C_4H_4NH, boiling point 130°C) to pyrrolidine (C_4H_8NH, boiling point 89°C). This configuration has three advantages:

1. The non-volatile liquid reactant is completely converted. This cannot be accomplished in a BSR in which the effluent is a liquid phase.
2. The catalyst remains in the reactor avoiding the expensive catalyst/liquid separation. While internal filtering with recycle may be used when catalyst attrition does not occur, in many applications the catalyst separation from the product is one of the difficult tasks involved in slurry reactor operation.
3. The use of expensive heat exchangers may be eliminated by feeding the reactor with a proper liquid (solvent) with a higher volatility than that of the liquid reactant. One possible choice of a solvent is a by-product formed by an irreversible reaction.

We have previously studied the behavioral features of a BSR in which a single reaction $A \rightarrow D$ occurs (Khinast et al., 1998). We study here situations in which in addition to the desired reaction an undesired simultaneous or consecutive reaction occurs. The goal is to determine if

*Corresponding author. Present address: Department of Chemical and Biochemical Engineering, Rutgers University, Piscataway, NJ 08854-8058, USA. Fax: 001 732 445 2581.
E-mail address: khinast@sol.rutgers.edu (J. Khinast).

0009-2509/99/$ – see front matter
PII: S0009-2509(98)00357-1

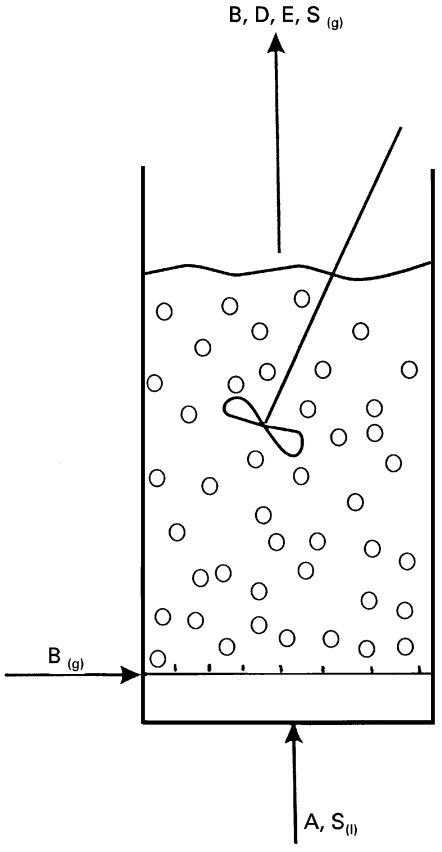

Fig. 1. Schematic diagram of the boiling slurry reactor (BSR).

and how the undesired reaction may affect the qualitative behavioral features of the reactor and the selectivity and yield of the reaction.

2. Mathematical model of the BSR

We consider a BSR in which both a desired and an undesired catalytic gas–liquid reaction occurs and study the influence of the undesired reaction on the reactor behavior. Two different cases are considered. The first when an undesired simultaneous reaction occurs, i.e.,

$$\mathrm{R}_1\colon\ \mathrm{A}+\mathrm{B}\rightarrow\mathrm{D}+\mathrm{S},\quad \mathrm{R}_2\colon\ \mathrm{A}+\mathrm{B}\rightarrow\mathrm{E}+\mathrm{S}. \tag{1}$$

The second when an undesired consecutive reaction occurs, i.e.,

$$\mathrm{R}_1\colon\ \mathrm{A}+\mathrm{B}\rightarrow\mathrm{D}+\mathrm{S},\quad \mathrm{R}_2\colon\ \mathrm{D}+\mathrm{B}\rightarrow\mathrm{E}+\mathrm{S}. \tag{2}$$

The non-volatile organic reactant (A) is dissolved in an inert volatile solvent (S). While the assumption that A is non-volatile is valid under normal operating conditions of the BSR, it may not be adequate at very high-temperature states. However, accounting for the volatility of the limiting liquid reactant under these conditions is not expected to affect the qualitative behavioral features under normal operating conditions. At steady state complete conversion of A has to be obtained to avoid its accumulation in the reactor. The gaseous feed is pure B. The heat generated by the exothermic reactions evaporates both the liquid products (D, E) and the solvent (S) and preheats the feed. The solid catalyst particles are dispersed by the gas in the liquid phase.

The molar balances of the five species (i = A, B, D, E, S) in the liquid phase are

$$\frac{\mathrm{d}(c_{i,l}V_l)}{\mathrm{d}t}=F^f_{i,l}-\dot{N}^t_i+\nu_{1,i}\rho_s V_s r_1+\nu_{2,i}\rho_s V_s r_2, \tag{3}$$

where $F^f_{i,l}$ is the molar feed rate of component i in the liquid. The stoichiometric coefficients of reactions (1) and (2) may be determined from Eqs. (1) and (2). The gas–liquid mass-transfer rates $\dot{N}^t_i$ are

$$\dot{N}^t_i=\begin{cases}0, & i=\mathrm{A},\\ V_l k_l a_v\left[c_{B,l}-\dfrac{p_B}{H_B(T)}\right], & i=\mathrm{B},\\ V_l k_l a_v\left[c_{i,l}-\dfrac{c_l y_i}{K_i(T)}\right], & i=\mathrm{D,E,S}.\end{cases} \tag{4}$$

In Eq. (4), y_i is the mole fractions of species i in the gas phase and c_l is the total molar liquid concentration. The reaction rate of the first reaction is

$$r_1=k_1(T_R)\exp\left[\frac{-E_1}{R}\left(\frac{1}{T}-\frac{1}{T_R}\right)\right]\frac{K_{\mathrm{ad},1}(T)c_A c_B}{1+K_{\mathrm{ad},1}(T)c_A}, \tag{5}$$

$$K_{\mathrm{ad},1}(T)=K_{\mathrm{ad},1}(T_R)\exp\left[\frac{-\Delta H_{\mathrm{ad},1}}{R}\left(\frac{1}{T}-\frac{1}{T_R}\right)\right].$$

The reaction rate of the second simultaneous reaction is

$$r_2=k_2(T_R)\exp\left[\frac{-E_2}{R}\left(\frac{1}{T}-\frac{1}{T_R}\right)\right]\frac{K_{\mathrm{ad},2}(T)c_A c_B}{1+K_{\mathrm{ad},2}(T)c_A},$$

$$K_{\mathrm{ad},2}(T)=K_{\mathrm{ad},1}(T). \tag{6}$$

Note, that the adsorption constant of A is identical for both reactions. For the undesired consecutive reaction the reaction rate is identical to Eq. (6) with c_A being replaced by c_D. The adsorption constant is assumed to be identical to that in the simultaneous case. Adsorption of B is assumed to be not rate limiting in both reaction networks. Finally, the sum of the liquid volume fractions of the components has to be unity,

$$c_{A,l}\hat{V}_A+c_{B,l}\hat{V}_B+c_{D,l}\hat{V}_D+c_{S,l}\hat{V}_S+c_{E,l}\hat{V}_E=1. \tag{7}$$

Table 1
Parameter values used in the simulations

Parameter	Value	Parameter	Value	Parameter	Value
A_R	1.8 m^2	$F^f_{D,l}$, $F^f_{B,l}$	0.0 kmol/s	T_R	453.0 K
$c_{p,s}$	1.1 kJ/kg/K	$\Delta H_{\mathrm{ad},1}$	−20 kJ/mol	T^f_l	373.0 K
$c_{v,l,A}$	100 kJ/kmol/K	$\Delta H^v_D(T_R)$	17.6 kJ/mol	T^f_g	453.0 K
$c_{v,l,B}$	50 kJ/kmol/K	$\Delta H^v_E(T_R)$	16.0 kJ/mol	T_0	298.0 K
$c_{v,l,D}$	80 kJ/kmol/K	$\Delta H^v_S(T_R)$	28 kJ/mol	u^t_b	0.23 m/s
$c_{v,l,E}$	80 kJ/kmol/K	$\Delta H^v_B(T_R)$	0 kJ/mol	$\hat{V}_A$	0.073 m^3/kmol
$c_{v,l,S}$	80 kJ/kmol/K	H_B	60 m^3 bar/kmol	$\hat{V}_B$	0.01 m^3/kmol
$c_{v,g,B}$	40 kJ/kmol/K	$k_1(T_R)$	0.0008 kmol/(s kg$_{\mathrm{cat}}$)	$\hat{V}_D$	0.081 m^3/kmol
$c_{v,g,D}$	40 kJ/kmol/K	$K_{\mathrm{ad},1}(T_R)$	20 m^3/kmol	$\hat{V}_E$	0.07 m^3/kmol
$c_{v,g,E}$	40 kJ/kmol/K	k_P	1.0 m^3/bar/s^2	$\hat{V}_S$	0.018 m^3/kmol
$c_{v,g,S}$	40 kJ/kmol/K	k_i	0.01 m^3/bar/s^2	V_S	2.5 m^3
E_1	80 kJ/mol	$k_l a_v$	0.1 s^{-1}	ρ_s	1500 kg/m^3
$F^f_{A,l}$	0.1 kmol/s	$\hat{P}$	20 bar		

Table 2
Reaction parameters

Parameter	Case 1 (simultaneous)	Case 2 (consecutive)
$k_2(T_R)$	$0.01k_1(T_R)$	$0.01k_1(T_R)$
E_2	$2.0E_1$	$2.0E_1$
$\Delta H_{r,1}$	−80 kJ/mol	−120 kJ/mol
$\Delta H_{r,2}$	$1.6\Delta H_{r,1}$	$0.5\Delta H_{r,1}$
$K_{\mathrm{ad},2}(T_R)$	$K_{\mathrm{ad},1}(T_R)$	$K_{\mathrm{ad},1}(T_R)$
$\Delta H_{\mathrm{ad},2}$	$\Delta H_{\mathrm{ad},1}$	$\Delta H_{\mathrm{ad},1}$

The molar gas-phase balances of the four volatile species (B, D, E S) are

$$\frac{1}{R}\frac{\mathrm{d}[p_i/T\cdot V_b]}{\mathrm{d}t} = F^f_{i,g} - F_g\frac{p_i}{P} + \dot{N}^t_i, \quad i = \text{ B, D, S, E.} \tag{8}$$

The overall energy balance is

$$\left(V_l\sum_i c_{i,l}c_{v,i,l} + \frac{V_b}{RT}\sum_i p_i c_{v,i,g} + V_s\rho_s c_{p,s}\right)\frac{\mathrm{d}T}{\mathrm{d}t}$$
$$= -\Delta H_{r,1}(T)\rho_s V_s r_1 - \Delta H_{r,2}(T)\rho_s V_s r_2$$
$$-\sum_i \dot{N}^t_i[\Delta H^v_i(T_0) + (c_{v,g,i} - c_{v,l,i})(T - T_0)]$$
$$-\sum_i F^f_{i,l}c_{v,i,l}(T - T^f_l) - \sum_i F^f_{i,g}c_{v,i,g}(T - T^f_g),$$
$$i = \text{A, B, D, S, E.} \tag{9}$$

A term accounting for the work required to increase the gaseous molar flow can be safely neglected in the energy balance. The reactor pressure control determines the effluent rate

$$\frac{\mathrm{d}(F_g/c_g)}{\mathrm{d}t} = k_p\frac{\mathrm{d}(P-\hat{P})}{\mathrm{d}t} + \frac{\mathrm{d}}{\mathrm{d}t}\left[k_i\int_0^t (P(s)-\hat{P})\,\mathrm{d}s\right]. \tag{10}$$

The holdup of the bubble phase is (Saxena, 1995)

$$\frac{V_b}{V_b + V_l + V_s} = \frac{u_g}{2.5u_g + u^t_b}, \tag{11}$$

where u^t_b is the terminal rise velocity of the bubble swarm. Saxena (1995) considers u^t_b to be a function of the slurry viscosity, the surface tension and the vapor pressure of the liquid. We assume a constant value for u^t_b. The mean superficial gas velocity u_g is computed by dividing the volumetric effluent rate F_g/c_g by the cross-section area A_r of the reactor. To reduce the number of parameters in the model we assume that the Henry constant in Eq. (4) is constant and not a function of temperature. The equilibrium constants K_i are given by

$$K_i = \frac{P_{v,i}}{P}. \tag{12}$$

The vapor pressures P_v of the components D, E and S are

$$\log(P_{v,D}) = 4.791 - 1717.4/T, \tag{13}$$

$$\log(P_{v,E}) = 4.905 - 1717.4/T, \tag{14}$$

$$\ln(P_{v,S}) = 5.4 + (1-z)^{-1}(-7.765z + 1.458z^{1.5} - 2.776z^3 - 1.233z^6), \quad z = 1 - \frac{T}{647.3}. \tag{15}$$

The parameter values used in the simulations for both reaction networks are given in Table 1. Those that fit only one reaction network are reported in Table 2.

The set of model equations consists of 16 dependent variables (five liquid concentrations, $c_{i,l}$, and four partial pressures p_i, V_l, V_b, P, c_g, T, F_g, u_g) which are described by 11 ODEs (Eqs. (3), (8), (9) and (10)) and two algebraic equations (Eqs. (7) and (11). Three additional algebraic relations are the ideal gas law, the sum of all partial pressures being equal to the total pressure, and $u_g = F_g/(c_g A_r)$. The independent variables, which may be

controlled are the feed rates and feed temperatures, i.e., $F^f_{A,l}$, $F^f_{S,l}$, $F^f_{B,g}$ and T^f_l, T^f_g. Note that the balance equations account neither for the total reactor volume nor for gas head volume. Thus, the model may predict that some steady-state operating conditions require unrealistically large slurry volumes. Clearly, one would not operate a BSR under these conditions.

We denote the gaseous/liquid feed ratio (B/A-ratio) as

$$\beta = \frac{\nu_A}{\nu_B}\frac{F^f_{B,g}}{F^f_{A,l}} = \frac{F^f_{B,g}}{F^f_{A,l}}. \tag{16}$$

A β value of unity is the minimum required for complete conversion of the non-volatile reactant A when a second consecutive reaction does not occur. Clearly, to obtain complete liquid reactant conversion and to avoid its accumulation β should exceed unity. The mole fraction of the reactant in the liquid feed is

$$x = \frac{F^f_{A,l}}{F^f_{A,l} + F^f_{S,l}}. \tag{17}$$

We shall now determine the steady-state behavior of the BSR and the conditions under which it may be attained, as well as some unique dynamic features of the BSR.

3. Simulation results

3.1. Undesired simultaneous reaction

We consider here a BSR in which the reaction heat and activation energy of the undesired reaction exceed those of the desired reaction. Thus, the undesired reaction is dominant at high temperatures. It is important to prevent a shift to these high-temperature states at which the yield of the desired product is low. Moreover, the corresponding high rate of heat release may lead to unsafe operation.

Fig. 2 describes the dependence of the steady-state temperature, the liquid volume and the corresponding "B-free" effluent mole fractions of the products on the feed mole fraction of the limiting liquid reactant A. The parameter is β, i.e., the molar ratio of gas-to-liquid reactants.

The simulations show that multiple steady states exist for some operating conditions in a bounded region of feed molar concentrations. The low- and high-temperature states are stable and the intermediate one is unstable. This multiplicity is not found in a BSR in which a single reaction occurs (Khinast et al., 1998) and is due to the presence of the second reaction. The yield of the desired product at the high-temperature states is low. Increasing the feed rate of the gaseous reactant B increases the range of the liquid reactant mole fraction for

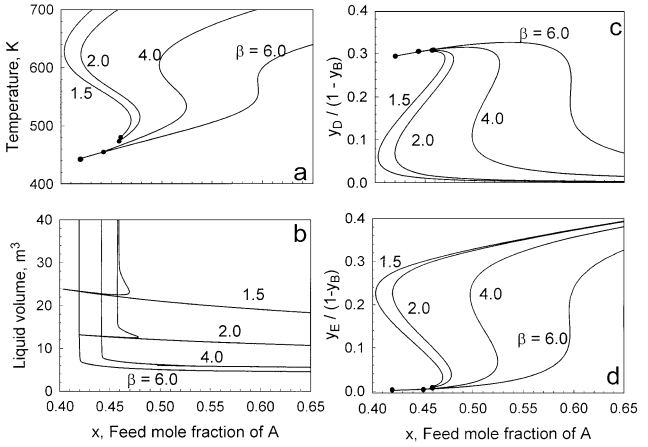

Fig. 2. Dependence of the (a) reactor temperature, (b) liquid volume (c) mole fraction of the desired product D and (d) undesired reaction product E in the effluent on the liquid reactant feed mole fraction and the gas to liquid reactant feed ratio β (simultaneous reactions case). In both cases $T^f_l = 373$ K and $T^f_g = 453$ K.

which a low-temperature, high-yield state exists and decreases the multiplicity region. Additionally, the temperatures of states on the high-temperature branch decrease significantly as the feed rate of the gaseous reactant B is increased.

Note that steady-state operation of the BSR is not feasible for very low feed mole fractions of the liquid reactant A. The branches of the feasible solutions emanate from a state (represented by a dot in Fig. 2), which we call the *heat generation limit* (Khinast et al., 1998). At this state the heat generated by the reaction is barely sufficient to evaporate the liquid solvent and products and the corresponding liquid volume is extremely large. Fig. 2b shows the drastic increase in the liquid volume as the heat generation limit is approached. This large slurry volume makes the operation next to this limit unpractical.

Under certain conditions the BSR may have in addition to the steady states two types of *pseudo-steady states*. In the first, referred to as a *fill-up state*, the reactor temperature and concentrations of all the species remain virtually constant, while the liquid volume increases monotonically. Clearly, this operation will eventually lead to a spill-over and require shut-down or a proper adjustment of the operating conditions. A simulation of a fill-up state is shown in Fig. 3a.

In the second pseudo-steady state, referred to as a *dry-up state*, the liquid volume decreases monotonically, while the other state variables remain unchanged. Eventually, the dry-up state becomes unstable and the system shifts to the closest steady state, or to a fill-up state if no feasible steady state exists. Fig. 3b describes such a shift to a steady state. The initial volume increase is caused by the initial temperature decrease as the feed is introduced into a reactor filled with pure solvent. This shift to

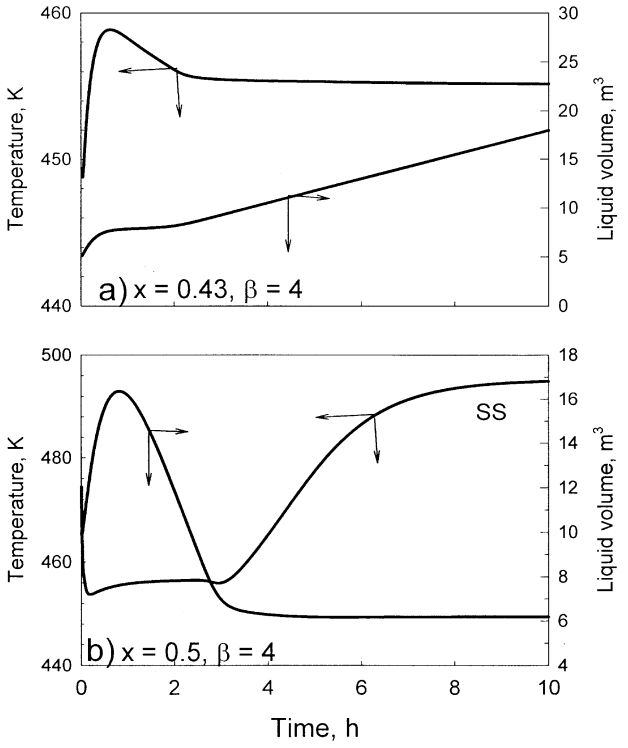

Fig. 3. Dynamic simulation of a (a) reactor fill-up state and (b) a dry-up state. In both cases $T_l^f = 373$ K and $T_g^f = 453$ K. The letters (a) and (b) also refer to states marked in Fig. 4.

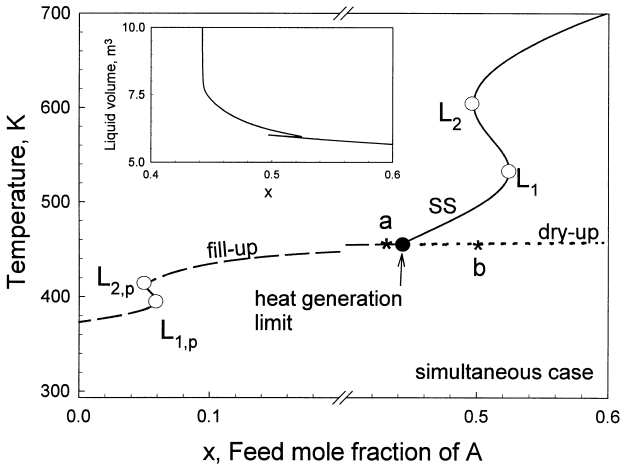

Fig. 4. Bifurcation diagram of the feasible steady states (solid line), fill-up states (dashed line), and dry-up states (short dashed line) as a function of the feed mole fraction of the limiting reactant A for $\beta = 4$, $T_l^f = 373$ K and $T_g^f = 453$ K. (L_i = limit point, $L_{i,P}$ = limit point of pseudo-steady states, SS = steady state). The inset is the steady-state liquid volume corresponding to the SS line.

a dry-up state may be prevented either by preheating the reactor contents before introducing the feed or by using initially a feed with higher temperature or by filling the reactor initially with a mixture of the reactant and the solvent.

Fill-up and dry-up states may be predicted by a pseudo-steady state model of the BSR, described in Appendix A, which accounts for a constant rate of change in the liquid volume. It should be noted that a fill-up and/or dry-up state may exist under conditions for which no feasible steady state exists. In this specific example a dry-up state exists only under the conditions for which a steady state solution exists. The branches of the steady-states, fill-up and dry-up states for $\beta = 4$ are shown in Fig. 4. A steady state exists for all $x > 0.44$, which is the heat generation limit. Multiple steady states exist for x values bounded by the two limit points L_1 and L_2. The dependence of the liquid volume on the feed reactant concentration x is shown in the inset. A marked increase in the liquid volume occurs close to the heat generation limit. While a dry-up state exists only for $x > 0.44$ a fill-up state exists only for $x < 0.44$, i.e., for feeds for which a steady state does not exist. It is of interest to note that multiple fill-up states exist for x values bounded by the two limiting points $L_{1,P}$ and $L_{2,P}$. Our simulations indicate that for other sets of parameters (single reaction case, Khinast et al., 1998) both a fill-up and steady states may coexist and the limit point $L_{1,P}$ is to the right of the heat generation limit. In such cases it is important to design a proper start-up procedure which avoids a shift to the fill-up state.

Fig. 5 shows the loci of the bifurcation points of both the steady-state and fill-up states. A cusp (H) of the multiplicity region exists at $x = 0.605$ and $\beta = 6.1$. Thus, no multiple steady states occur for higher values of either x or β. The figure includes also (dashed line) the locus of the heat generation limit. Feasible steady states exist only for x values to the right of the heat generation limit and β values exceeding 1. Fig. 5 includes the locus of the operating conditions at which the selectivity of the desired product $Y = p_D/(p_D + p_E)$ is 90%. A lower selectivity is obtained for operation to the right of this locus. Similar curves can be constructed for other specified selectivity levels. Such a map is very useful for selecting the desired feed concentrations. The multiplicity region of the fill-up states, bounded by the loci of $L_{1,P}$ and $L_{2,P}$ is mainly of academic interest in this problem as it occurs outside the feasible steady-state region. This, however, is not always the case as shown in a previous study for a different choice of reaction parameters (Khinast et al., 1998).

3.2. Undesired consecutive reaction

A BSR in which a consecutive undesired reaction occurs exhibits some unique features, which differ from those when an undesired simultaneous reaction occurs. The bifurcation diagrams of the steady-state temperature, liquid volume, $y_D/(1 - y_B)$ and $y_E/(1 - y_B)$ shown in Fig. 6 are qualitatively similar to those of the undesired simultaneous reaction for all $\beta > 2$. Again, steady-state

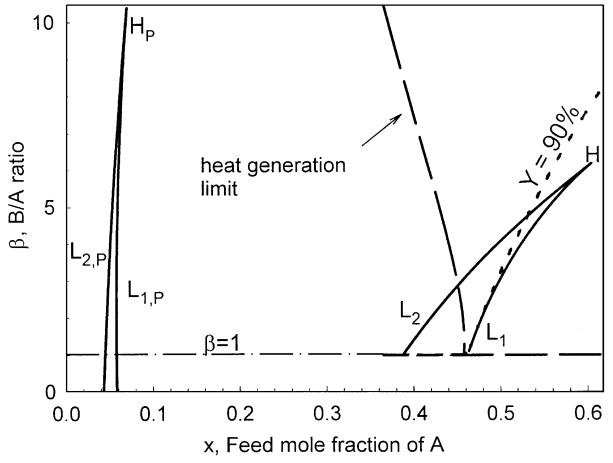

Fig. 5. Feasibility map showing the limit points, $Y = 90\%$ curve, heat generation limit and the limit points of the pseudo-steady-state model. Operation is only feasible to the right of the heat generation limit, for $\beta > 1$ and to the left of L_1 (H = hysteresis points, H_P = hysteresis of the pseudo-steady-state limit points, L = limit points, $L_{i,P}$ = limit points of the pseudo-steady-state model).

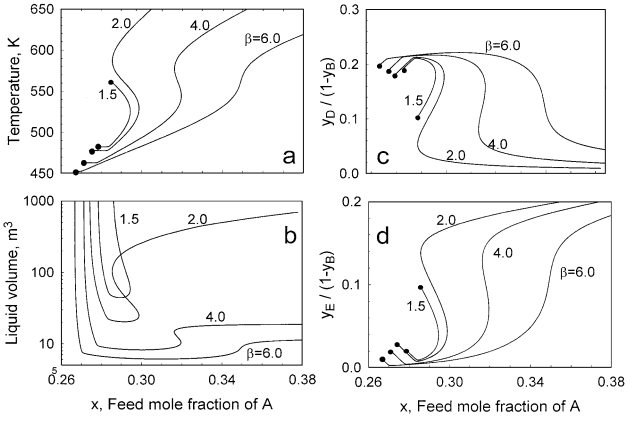

Fig. 6. Dependence of the (a) reactor temperature, (b) liquid volume (c) mole fraction of the desired product D and (d) undesired reaction product E in the effluent on the liquid reactant feed mole fraction and the gas to liquid reactant feed ratio β (consecutive reactions case). In both cases $T_l^f = 373$ K and $T_g^f = 453$ K.

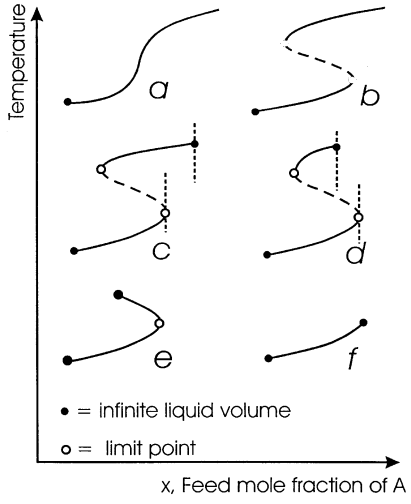

Fig. 7. Schematic bifurcation diagrams of the steady states temperature vs. feed mole fraction of the liquid reactant A for different B/A ratios β (consecutive reaction case). (solid lines = stable steady states, dashed line = unstable steady states).

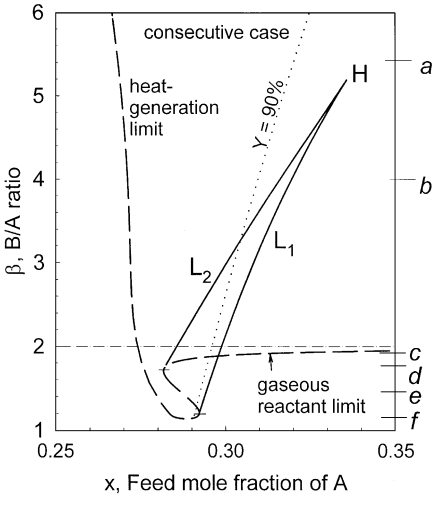

Fig. 8. Map showing the limit points, the loci of $Y = 90\%$, the heat generation and the gaseous reactant limit for the consecutive reaction case. Operation is only feasible to the right of the heat generation limit, for $\beta > 1$ and to the left of L_1 and the gaseous reactant limit. Letters at the ordinate correspond to the schematic bifurcation diagrams in Fig. 7. (H = hysteresis points).

multiplicity occurs for a bounded range of x values for not too high β values. An increase in β increases the range of x values for which a steady-state with a high yield of the desired product is obtained, decreases the required slurry volume, and decreases the range of x values for which steady-state multiplicity occurs. For any β value a feasible steady-state solution does not exist for x values smaller than that of the heat generation limit, at which the required liquid volume is unbounded. The model predicts that for all $\beta < 2$ ($\beta = 2$ is the amount of B needed to completely convert A to the undesired product E) there exists also a *gaseous reactant limit* (marked as a black dot at the high-temperature branch in Fig. 6a) at which all the gaseous reactant B is completely depleted by the two reactions. Since the gas-phase concentration of B becomes negligible at this state a very large interfacial area and hence slurry volume is needed to enable complete absorption and consumption of B (low mass-transfer driving force). Thus, the feasible steady-state branches for $\beta < 2$ are bounded by two limiting states with very large liquid volumes (Fig. 6b). Note that using $\beta < 2$ prevents the reactor from shifting to states with very low yield of the desired product due to its complete consumption by the undesired reaction.

Six qualitatively different bifurcation diagrams of the steady-state temperature vs. the liquid feed concentration

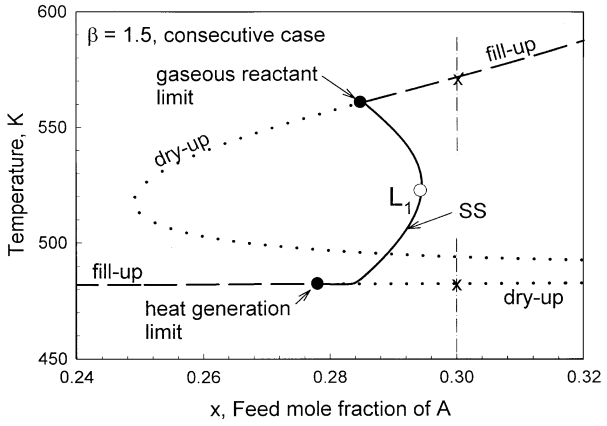

Fig. 9. Bifurcation diagram of the feasible steady states (solid line), fill-up states (dashed line), and dry-up states (short dashed line) of the consecutive reaction case as a function of the feed mole fraction of the limiting reactant A for $\beta = 1.5$. (L = limit point, SS = steady-state).

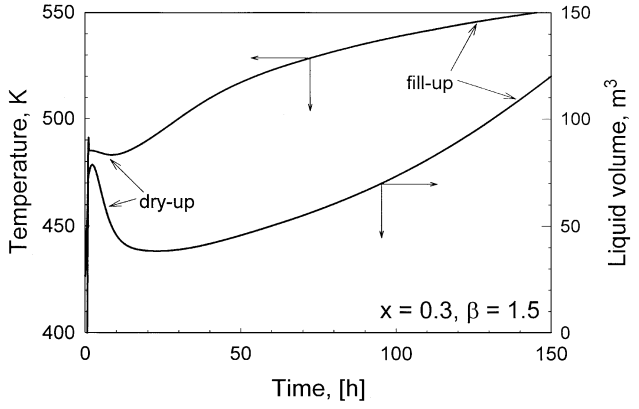

Fig. 10. Dynamic simulation of the BSR for $x = 0.3$ and $\beta = 1.5$ for the consecutive reaction case. First a dry-up state and then a reactor fill-up state is obtained. The states of the reactor are marked as "x" in Fig. 9.

exist in the consecutive case (Fig. 7). The first two diagrams (cases a and b) are for $\beta > 2$ and are qualitatively similar to those obtained for the simultaneous reactions case. The other four cases (c–f) are for $\beta < 2$ and consist of branches, which terminate at two limiting points (heat generation and gaseous reactant limit) with very large liquid volume. In case c, multiple steady states exist which are bounded by the heat generation and gaseous reactant limit. At the transition from case c to d the ignition point and the gaseous reactant limit interchange their relative position. In case e the extinction point and in case f also the ignition point vanish since the gaseous reactant limit moves towards the heat generation limit. Below $\beta = 1.15$ (coalescence of the heat generation and gaseous reactant limit) no steady states exist. No similar diagrams exist for the simultaneous reaction case. The development of these six bifurcation diagrams can be understood by inspection of Fig. 8. It describes the loci of the limit points L_1 and L_2, the loci of the heat generation and gaseous reactant limits, and the operating parameters at which a selectivity $Y = 90\%$ of the desired product is obtained (short dashed line). Note, that heat generation and gaseous reactant limit form one curve. The bifurcation diagrams in Fig. 7 correspond to β values denoted by the same letters on the ordinate of Fig. 8. The short horizontal lines for $\beta < 2$ are the boundaries of qualitatively different types of bifurcation diagrams.

For β values larger than 2 the qualitative features of the map of the limit points and heat generation limit points of the consecutive reaction model are very similar to that of the simultaneous reaction (Fig. 5). Multiplicity of the steady states does not occur for either β or x values exceeding that of the cusp H formed by the intersection of the limit points. Similarly, for $\beta > 2$ fill-up states exist only to the left of the heat generation limit, i.e., for x values for which no steady state exists.

However, the qualitative behavioral features may change drastically for $\beta < 2$ due to the emergence of the multiplicity of the dry-up states and the existence of a branch of fill-up states for x values exceeding the gaseous reactant limit. A typical case is shown in the bifurcation diagram of Fig. 9, which includes a segment of the branches of the dry-up and fill-up states in addition to the feasible steady-state branch. (The figure does not include the limit points of the fill-up states, which exist for $x < 0.1$, and of a limit point of the dry-up states, which exists for $x > 0.32$.) Note, that the steady states between L_1 and the gaseous reactant limit are unstable.

Simulations show that the region of attraction of the low- and high-temperature dry-up states between the limit point L_1 of the steady-state branch and the heat generation limit is rather small. Moreover, even if a stable dry-up state is attained the reactor eventually shifts to the steady state. However, when the initial conditions lead to a fill-up state for x values exceeding the gaseous reactant limit point a shift to a feasible steady state requires a proper change in the feed conditions.

For x values to the right of the limit point L_1 of the steady-states branch and to the left of the limit point of the dry-up states (not shown in Fig. 9) a stable dry-up state and a stable fill-up state coexist. Fig. 10 shows the dynamic behavior for such a case ($x = 0.3$) when the reactor contained initially a pure solvent at 373 K. At first, the slurry volume increases as the heat of the reaction is not sufficient to evaporate the products and solvent (initially pure solvent). After about 1.5 h (the liquid reactant residence time in the reactor is of the order of 1 h) the reactor shifts to a dry-up state and its volume decreases monotonically. It shifts later to a fill-up state, which will eventually lead to a spill-over if no change in the feed conditions will be implemented. Operation in this region may lead to unexpected pitfalls and surprises if a model predicting these states is not available.

4. Conclusions and remarks

The proposed BSR configuration offers several advantages over conventional slurry reactors. It enables complete conversion of the liquid reactant, while conventional slurry reactors require a much larger volume to approach complete conversion. Moreover, the BSR does not require an expensive solid–liquid separation, which complicates the operation of many slurry reactors. Additionally, no internal or external cooling devices are required since the reactor is cooled by evaporation of the solvent and the liquid products.

The existence of an undesired simultaneous or consecutive reaction in addition to the desired one may lead to qualitative changes in the behavior of a BSR. The undesired reaction may cause the existence of three steady-state solutions, two of which are stable, while only a unique steady state exists in the absence of the undesired reaction. One of the two stable steady states needs to be avoided due to its low yield of the desired product and excessive temperature rise. Use of a large excess of the gaseous reactant decreases the range of x values for which steady-state multiplicity exists and eventually eliminates its occurrence. Moreover, increasing β expands the range of liquid feed concentrations for which a high-yield state is obtained. The consecutive reaction case leads to a larger variety of dynamic features than does the simultaneous reaction case. Also, in the case of a consecutive undesired reaction a β value less than two may be used to eliminate the possible complete conversion to the undesired product and the corresponding high temperature rise.

The existence of dry-up and fill-up states is a unique surprising feature of the BSR. Their existence can increase significantly the sensitivity of the start-up procedure on the initial conditions. Careful reactor start-up is required in the case of the consecutive reaction with $\beta < 2$ since both fill-up and dry-up states may coexist with the steady states as well as for x values for which steady-state operation is not feasible. These pseudo-steady states may lead to severe pitfalls and frustration during the process and control policy development. Khinast et al. (1998) showed that the BSR model may predict oscillations for very unrealistic sets of parameters. In this study no oscillatory states were found for realistic values of the feed rates and temperatures.

Notation

a_v	gas liquid interfacial area per unit liquid volume, 1/m
A_R	reactor cross section area, m^2
c	molar concentration, kmol/m^3
c_v	heat capacity, kJ/(kmol K)
E	activation energy, kJ/kmol
F_i^f	feed rate of component i, kmol/s
F_g	molar effluent rate of gas phase, kmol/s
ΔH_r	heat of reaction, kJ/kmol
ΔH_{ad}	heat of adsorption, kJ/kmol
ΔH^v	heat of evaporation at T_R, kJ/kmol
H	Henry's law constant, m^3 bar/kmol
$k_l a_v$	volumetric mass transfer coefficient, 1/s
k_0	frequency factor, $m^3/(s\ kg_{cat})$
k_i	integral control constant, $m^3/(bar\ s^2)$
k_P	proportional control constant, m^3/(bar s)
K	gas–liquid equilibrium constant
K_{ad}	adsorption constant, m^3/kmol
$\dot{N}^t$	molar phase transfer rate (dissolution, evaporation), kmol/s
p	partial pressure, bar
P	system pressure, bar
P_v	vapor pressure, bar
$\hat{P}$	set point of system pressure, bar
r	reaction rate, kmol/(s kg_{cat})
R	universal gas constant
t	time, s
T	reactor temperature, K
u_g	mean superficial gas velocity, m/s
u_b^t	terminal rise velocity of the bubble swarm, m/s
V	phase volume, m^3
$\dot{V}$	rate of volume change, m^3/s
$\hat{V}$	molar volume, m^3/kmol
x	mole fraction of component A in the feed
y	mole fraction in the gas phase
Y	selectivity of the desired product $(=p_D/(p_D + p_E))$

Greek letters

β	B/A ratio
v	stoichiometric coefficient
ρ_s	density of solid catalyst, kg/m^3

Subscripts

b, g, l, s	bubble, gas, liquid, solid phase
R	reference

Superscripts

f	feed
v	vaporization

Appendix A. Pseudo-steady-state model

The reactor temperature and the concentrations approach asymptotically constant values during the reactor fill-up or dry-up states. The remaining variables (temperature and concentrations) remain essentially

unchanged and may be computed by using a pseudo-steady state model. This model is derived by assuming a large liquid volume ($V_l \gg 0$) and a constant rate of increase in the liquid volume ($\mathrm{d}V_l/\mathrm{d}t = \dot{V}_l = \text{const.}$). Under these conditions, equilibrium between the gas and liquid phase exists. Therefore, combined liquid–gas mass balances may be set up, i.e.,

$$F_{i,l}^f + F_{i,g}^f + \nu_{i,1}\rho_s V_s r_1 + \nu_{i,2}\rho_s V_s r_2 = \dot{V}_l c_i + \dot{V}_b \frac{p_i}{RT} + F_g \frac{p_i}{\hat{P}}, \quad i = \mathrm{A, B, D, S, E.} \tag{A.1}$$

Note, that $p_A = 0$. Due to the equilibrium, we have

$$p_B = H_B c_B, \quad p_D = P_v \frac{c_D}{c_l}, \quad p_E = P_{v,E} \frac{c_E}{c_l}, \quad p_S = P_{v,S} \frac{c_S}{c_l}. \tag{A.2}$$

The energy balance is

$$\sum_i F_{i,l}^f c_{v,i,l}(T_l^f - T_0) + \sum_i F_{i,g}^f (\Delta H_i^v(T_0) + c_{v,i,g}(T_g^f - T_0)) - \Delta H_{r,1}\rho_s V_s r_1 - \Delta H_{r,2}\rho_s V_s r_2 = \sum_i F_g \frac{p_i}{\hat{P}}(\Delta H_i^v(T_0) + c_{v,i,g}(T - T_0)) + \dot{V}_l \sum_i c_{i,l} c_{v,i,l}(T - T_0) + \dot{V}_b \sum_i \frac{p_i}{RT}(\Delta H_i^v(T_0) + c_{v,i,g}(T - T_0)), \quad i = \mathrm{A, B, D, E, S.} \tag{A.3}$$

An additional required relation is that the sum of the partial liquid volumes is unity, (Eq. (7)). Furthermore, the sum of the partial pressures equals the total pressure and the changes in the bubble and liquid volumes satisfy the relation

$$\dot{V}_b = \frac{u_g}{1.5u_g + u_b^t} \dot{V}_l, \tag{A.4}$$

which was obtained by differentiation of Eq. (11). The limiting model has nine variables (c_A, c_B, c_D, c_E, c_S, F_g, T, $\dot{V}_l$, $\dot{V}_g$) and is described by the nine equations given above.

References

Beenackers, A.A.C.M., & van Swaaij, W.P.H. (1986). Chemical reactor design and technology. In H.I. DeLasa (Ed.), *NATO Advanced Study Institute Series* (pp. 463–538). Dordrecht: Martinus Nijhoff.

Fan, L.S. (1989). *Gas–liquid–solid fluidization engineering*. Boston: Butterworths.

Gianetto, A., & Silveston, O.L. (1986). *Multiphase chemical reactors*. Washington, DC: Hemisphere Publishing Corp.

Hammer, H., Kusters, U., Schrag, H.J., Soemarno, A., Sahabi, U., Schonau, H., & Napp, U. (1984). In L.K. Doraiswamy (Ed.), *Recent advances in the engineering analysis of chemically reacting systems* (pp. 379–395). New Delhi: Wiley India.

Khinast, J., Luss, D., Leib, T.M., & Harold, M.P. (1998). The boiling slurry reactor: Feasible operation and stability. *A.I.Ch.E. J.*, *44* (8), 1868–1879.

Krishna, R., & Ellenberger, J. (1995). A unified approach to the scale-up of fluidized multiphase reactors. *Trans. I. Chem. E.*, *73* (A), 217–221.

Luyben, W.L. (1966). Stability of autorefrigerated chemical reactors. *A.I.Ch.E.J.*, *12* (4), 662–668

Ramachandran, P.A., & Chaudhari, R.V. (1983). *Three phase catalytic reactor*. New York: Gordon & Breach Science Pub.

Saxena, S.C. (1995). Bubble column reactors and Fischer–Tropsch synthesis. *Catal. Rev.-Sci. Engng*, *37* (2), 227–309.

Shah, Y.T. (1979). *Gas–liquid–solid reactor design*. New York: McGraw-Hill.